https://doi.org/10.5194/egusphere-2025-3487
Preprint. Discussion started: 16 September 2025

Tectonic control and geometric characterization of hydrothermal vent complex using seismic data, Potiguar Basin – Brazil

Lorenna Sávilla Brito Oliveira[1], Luiza Cavalcante Vinhas Lucas[1], David Iacopini[2], Fabrizio Balsamo[3], Anita Torabi[4], Behzad Alaei[5], João Felipe de Sousa Neto[1], Pedro Edson Face Moura[6], David Lino Vasconcelos[7], Vincenzo La Bruna[1], Francisco Hilário Rego Bezerra[1]

1 Postgraduate Program in Geodynamics and Geophysics, Federal University of Rio Grande do Norte (UFRN), Campus Universitário - Lagoa Nova, CEP 59078-970, Natal, Rio Grande do Norte, Brazil.

2 Department of Earth, Environmental and Resource Sciences (DISTAR - Dipartimento di Scienze della Terra, dell'Ambiente e delle Risorse), University of Naples Federico II, Naples, Italy.

3 Department of Chemistry, Life Sciences, and Environmental Sustainability, University of Parma, Parma, Italy.

4 Department of Geosciences, University of Oslo, Postboks 1047, Blindern 0316, Oslo, Norway.

5 Earth Science Analytics, Strandveien 3333, 1366 Lysaker, Norway.

6 Postgraduate Program in Geology, Federal University of Ceará (UFC), Campus do Pici, Bloco 912, CEP 60440-900, Fortaleza, Ceará, Brazil.

7 Federal University of Campina Grande (UFCG), Aprígio Veloso, 882, Campus Universitário, Campina Grande, Paraíba, CEP 58429-900, Brazil.

Correspondente to: Lorenna Oliveira (lorenna_savilla@hotmail.com)

ABSTRACT

Hydrothermal vent complexes in sedimentary basins are linked to igneous intrusions, which induce structural and thermal perturbations, causing forced folds, hydrocarbon maturation, and fluid remobilization. While their genesis is often associated with magmatic heat and hydraulic fracturing, the controlling factors of their geometry and development remain debated. This study analyzes 3D seismic data from the Potiguar Basin (onshore Brazil), identifying vent structures, two of which were extracted in a 3D perspective from the variance attribute. Our results indicate that all the vents are structurally controlled by regional-scale faults, which enhance permeability starting from the hydraulic

https://doi.org/10.5194/egusphere-2025-3487
Preprint. Discussion started: 16 September 2025

fracturing and boiling processes. Seismic attributes, such as variance and dip illumination have proven effective in identifying vent structures, fault associations, and fluid pathways, providing insights into their spatial distribution and geometric characteristics. Cosine of phase attribute reveals that hydrothermal vents exhibit varying geometries as they cut different sedimentary units within the basin. Our findings highlight the petrophysical implications of a fault zone in a hydrothermal vent complex and advance understanding of silicification processes in sedimentary reservoirs.

Keywords: Hydrothermal vents, seismic attributes, fault zones, fluid migration, sedimentary basins.

1. INTRODUCTION

Hydrothermal vents are a complex combination of elements that potentially affect the petrophysical properties of reservoirs. They have been described in sedimentary basins associated with volcanic activities as injections of igneous plumbing systems, dikes, and sills (Skoseid et al., 1992; White and McClintock, 2001; Svensen et al., 2003; Jamtveit et al., 2004; Planke et al., 2005; Hansen et al., 2008). These igneous injections are known to induce structures as forced folds, hydrofracturing systems, and seals. They also behave as hydrocarbon traps (Hansen and Cartwright, 2006; Jackson et al., 2013), causing early maturation of hydrocarbons (Kennish et al.,1992; Hansen and Cartwright, 2006), increasing the hydrothermal aureole width (Svensen et al., 2004), and remobilizing sand and fluid pipes (Svensen et al., 2006; Jamtveit et al., 2004). All these volcanic processes create disturbances in the reservoirs, forming hydrothermal vents with various architectures that relocate gas, mixed fluids, and

https://doi.org/10.5194/egusphere-2025-3487
Preprint. Discussion started: 16 September 2025

hot waters (Svensen et al., 2003; Procesi et al., 2019; Finn et al., 2022; Rovere et al., 2022).

The hydrothermal vents are associated with igneous intrusions. However, the intrusive processes and rock parameters that control the pathways and conduit architectures of these structures remain poorly understood, as most interpretations are based on post-mortem seismic data analysis (Cartwright, 2010; Jamtveit et al., 2004; Planke et al., 2005; Svensen et al., 2006; Moss and Cartwright, 2010b). The major uncertainty refers to what triggers the hydraulic fracturing mechanisms that guide the nucleation and then propagation of the vent formation. Other than intrusive systems, hydrothermal vents have been described as developed by synsedimentary processes, or erosive fluidization (McDonnell et al., 2007). Depending on the type of sills, intrusions trigger the overpressure region (Svensen et al., 2006; Davies et al., 2012; Alvarenga et al., 2016). Other uncertainties relate to the vent interactions with the seabed cap depending on its geological nature and stratigraphy (Moss and Cartwright, 2010b).

In vent complexes, the main pathways have been described by fluid escape structures named fluid pipes, characterized by highly localized vertical to sub-vertical pathways of focused fluid venting from some underlying source region. The term fluid pipe was used as synonymous of gas chimney triggered by a pressure cell, composed of a gas or mud source (Svensen et al., 2006). In literature, the geometry of vents (both methane or hydrothermal) has been classified based on cross-sectional and plan-view characteristics as dome-shaped, eye-shaped, and crater forms (Planke et al., 2005; Cartwright and Santamarina, 2015) (Fig. 1B). The relationship between vent boundaries and surrounding strata have been defined, focusing on concordant, divergent, or

https://doi.org/10.5194/egusphere-2025-3487
Preprint. Discussion started: 16 September 2025

truncated patterns (Fig. 1B), but also using the internal reflections within vents (Hansen, 2006). In seismic data, vents (no matter their origin) can be measured by the diameters and lengths of conduits, checking the connections between sill terminations and upper vent regions identified as cylindrical zones of disturbed seismic data (Hansen, 2006; Maestrelli et al., 2017) (Fig. 1A and Fig. 1C).

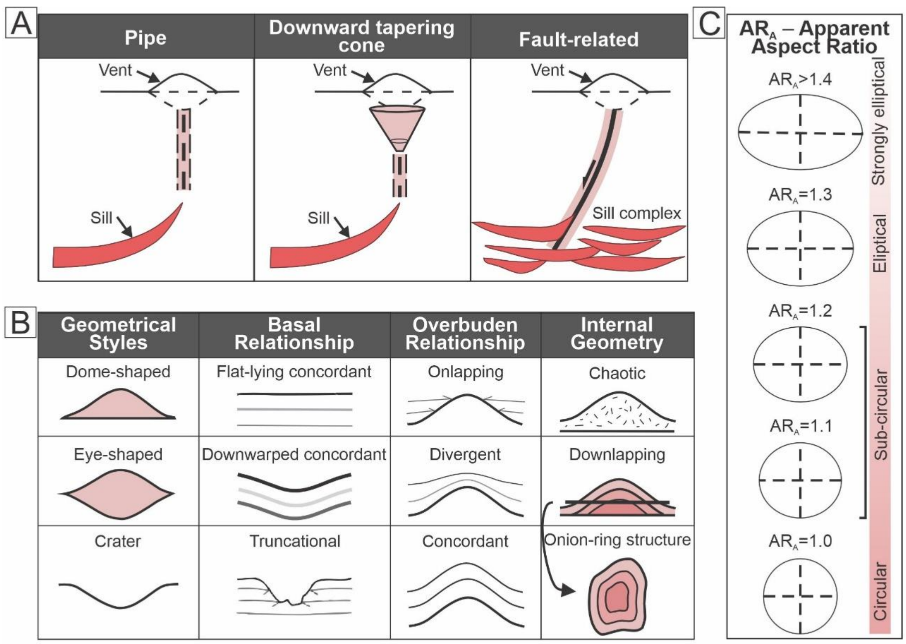

Figure 1 - Vent geometric parameters related to the external (A) and internal (B) shapes and the Apparent Aspect Ratio classification (C) related to the pipes ratio in a map view, which expresses the variation between circular to strongly elliptical shapes. (A), (B) and (C) were modified from Hansen et al (2006), Planke et al (2005), and Maestrelli et al (2017).

In all those contexts, seismic data represent a useful tool for identifying hydrothermal vents in several sedimentary basins (Planke et al., 2005; Hansen, 2006; Cartwright and Santamarina, 2015; Alvarenga et al., 2016; Kjoberg et al., 2017; Omosanya et al., 2018; Wang et al., 2019; Mituku and Omosanya, 2020).

https://doi.org/10.5194/egusphere-2025-3487
Preprint. Discussion started: 16 September 2025

Seismic attributes have been applied to reveal hydrothermal chimneys, vents, and structures around them, such as faults, fractures, folds, and sag structures (Jackson et al., 2013; Plaza-Faverola et al., 2015; Omosanya et al., 2018; Rovere et al., 2022). Vents associated with preexisting structures have also been previously described as ducts forming at the tops of faults and classified as the 'fault-related' (Hansen, 2006; Maestrelli et al., 2017; Wang et al., 2019). These vents typically exhibit a vertical pipe-like shape with a dome or mound at the top (Alvarenga et al., 2016; Magee et al., 2016). Coherence attributes and instantaneous phase were used to highlight the sag collapse structures associated with polygonal faults, vents related to crestal faults, and fault-controlled vents (Hansen, 2006; McDonnell et al., 2007; de Mahiques et al., 2017; Omosanya et al., 2018; Mituku and Omosanya, 2020). However, these attributes applied as tools for identifying vent complex geometry failed to recognize lateral fluid injection features and hydrofractures.

Across several hydrothermal vent complexes, the mechanisms of propagation and the processes of nucleation remain poorly understood. Key scientific uncertainties include whether hydrothermal vent propagation is linked to preexisting fault zones, the extent to which the final architecture is controlled by fault systems, and whether some hydrothermal vents are entirely dependent on overpressure-driven intrusive mechanisms. Another important consideration is whether fault zones can later re-exploit the existing architecture of hydrothermal vents. Additionally, the influence of host rock properties on the development of vent architecture remains an open topic for investigation.

To answer the above questions, we selected the onshore part of the Potiguar Basin, where previous studies identified outcrops with hydrothermal

https://doi.org/10.5194/egusphere-2025-3487
Preprint. Discussion started: 16 September 2025

silicification related to faults (Menezes et al., 2019). This study aims to describe and characterize the architecture and surrounding structures of hydrothermal vents using 3D onshore seismic data from the Potiguar Basin. We identified and seismically characterized 3 hydrothermal vents and 9 fluid pipes using seismic attributes and extracted geobodies from 2 of them to better interpret their internal architecture. Our interpretations suggest that all the hydrothermal vents are associated with regional-scale faults, with their lateral extensions related to fluids affecting sedimentary formations. The mapped structure suggests faults provide the structural permeability, enhanced by the hydraulic fracturing, and leading to the formation of hydrothermal vents. The result of this study contributes to a better understanding of the hydrothermal vent propagation mechanism and silicification process in sedimentary successions.

2. GEOLOGICAL SETTINGS

The Potiguar Basin is situated in the Brazilian Equatorial Margin (Pessoa Neto et al., 2007) (Fig. 2). This passive margin basin formed during the Early Cretaceous and exhibits a structural framework characterized by half-grabens and horsts bounded by fault systems that reactivated shear zones in the crystalline basement (Matos, 1992, 1999; de Castro et al., 2012). Its evolution comprises three main depositional supersequences: rift, post-rift, and drift, corresponding to distinct tectono-sedimentary phases (Bertani et al., 1990; Pessoa Neto et al., 2007).

https://doi.org/10.5194/egusphere-2025-3487
Preprint. Discussion started: 16 September 2025

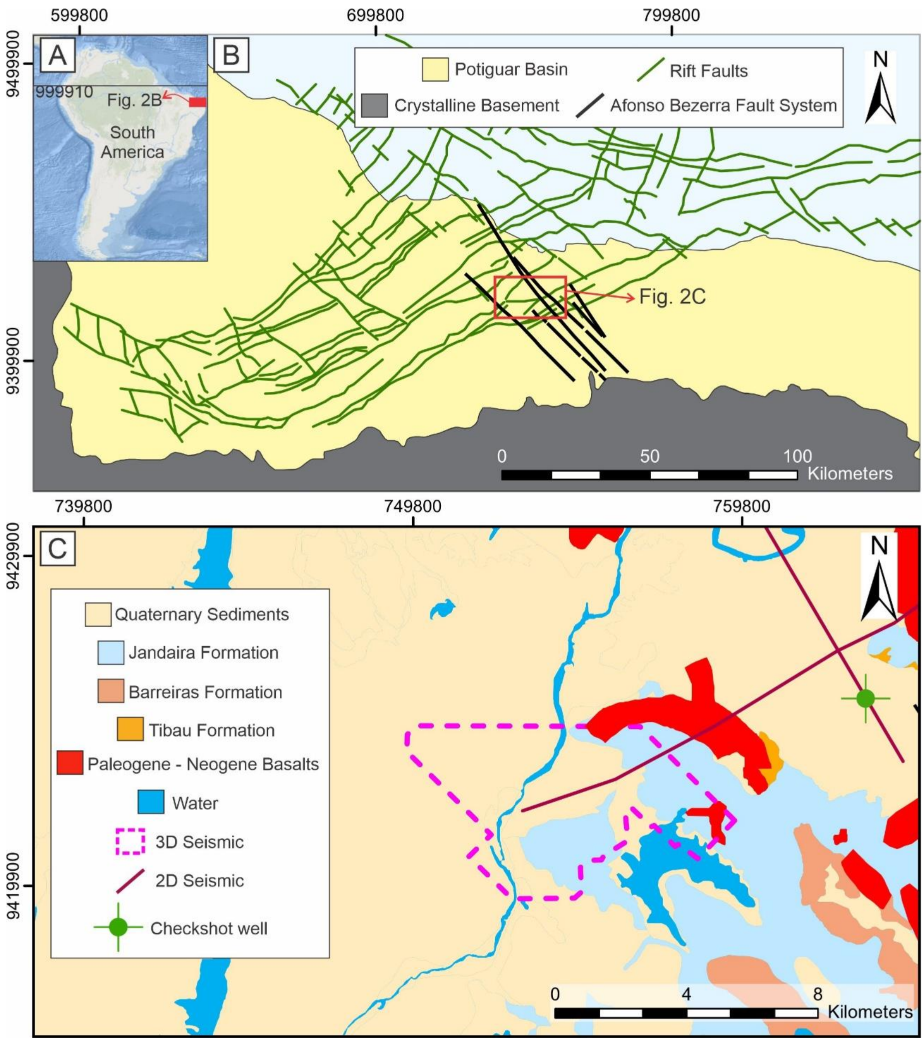

Figure 2 - (A) Study area located on the South American continent. (B) Geological map of the Potiguar Basin and (C) the study area with lithologies, and the seismic and well data location. Modified from Bertani et al. (1990), Bezerra et al. (2009), de Castro and Bezerra (2015).

The Potiguar basin rift phase coincides with the initial breakup of Pangea and the opening of the South Atlantic (de Castro, 2011; de Castro et al., 2014). This phase began during the early Valanginian, a stage characterized by intense crustal stretching, resulting in mechanical subsidence and the formation of

https://doi.org/10.5194/egusphere-2025-3487
Preprint. Discussion started: 16 September 2025

grabens (Araripe and Feijó, 1994; Fonseca et al., 2024). In this phase, the main structure was the Carnaubais fault system, striking NE-SW and dipping E-W, which resulted from the brittle reactivation of the Portalegre shear zone in the basement (de Castro et al., 2012). The creation of grabens and horsts is related to NE-SW-oriented linear features (Bertani et al., 1990). NW–SE-oriented transfer and accommodation faults controlled the southern edge of the rift, displacing the NE-SW-oriented faults in the Potiguar basin (de Castro et al., 2012), such as the Afonso Bezerra Fault System (ABFS). The sedimentary deposits formed during the rift phase varied from fluvial, lacustrine, and fan-deltaic (from the Pendências Formation) to deltaic and fluvio-deltaic units (from the Alagamar Fm) (Araripe and Feijó, 1994; Pessoa Neto et al., 2007).

The post-rift stage occurred in the early Albian, resulting from the breakup and opening of the seafloor (Fonseca et al., 2024). This stage involves thermal subsidence and the deposition of continental and marine sediments from the Alagamar Fm (Pessoa Neto et al., 2007). During the early Albian–Holocene, the drift phase was characterized by reduced subsidence rates driven by thermal and isostatic mechanisms (Bertani et al., 1990). This last stage included transgressive and regressive marine deposits (the Campanian-Maastrichtian Açu Fm), and represents the transition from fluvial-estuarine to marine environments, overlaid by the tidal-dominated carbonate shelf (the Turonian–Campanian Jandaíra Fm) (Pessoa Neto et al., 2007). The major unconformity marks the shift to transgressive deposits, which include the Barreiras, Tibau, Guamaré, and Ubarana formations, composed of siliciclastic to carbonate units (Pessoa Neto et al., 2007). These deposits reflect environments ranging from coastal fans, shallow platforms, and slope settings (Araripe and Feijó, 1994). The Afonso

https://doi.org/10.5194/egusphere-2025-3487
Preprint. Discussion started: 16 September 2025

Bezerra fault exhibits strike-slip and normal kinematics, affecting the rift and post-rift units, where circulation of Si-rich fluids occurred (Menezes et al., 2019).

Three significant magmatic events shaped the basin: Rift-related dikes date back to ~132 Ma (Pessoa Neto et al., 2007), while alkaline basalt spills from the Cuó Volcanism occurred around ~93 Ma (Souza et al., 2004); and during the Eocene/Oligocene the Macau Fm that represents later intrusions striking to N-S (50–6 Ma) (Souza et al., 2019).

On the surface of our study area, the top of the pipes structures was described before as a silicified fault zone (ABFS segment) in the lower carbonate unit of the Potiguar Basin. This fault zone is complex and wide (up to 800 m), featuring multiple episodes of silicification and brecciation. The silicified zone includes partially silicified areas (angular fragments in a non-silicified carbonate matrix) and fully silicified zones; the latter are subdivided into low-porosity (no vugs) and high-porosity (with centimeter-scale vugs along fractures) sections. Silicification completely replaced the carbonate mineralogy with quartz, chalcedony, and opal, significantly increasing SiO_2 content (from 3–15% to 94–97%) (Menezes et al., 2019). This study highlighted the heterogeneity of the fault zone, where dynamic (syn-tectonic) and static (non-deformational) silicification processes coexist, influencing reservoir quality.

3. DATA AND METHODS

3.1 DATA

https://doi.org/10.5194/egusphere-2025-3487
Preprint. Discussion started: 16 September 2025

The study area encompasses 57 km² of the onshore Potiguar Basin (Fig. 2B). Subsurface data, including seismic and well logs, were provided by the National Agency for Petroleum, Natural Gas, and Biofuels (ANP). We used seismic reflection data from a 3D seismic survey and two 2D seismic lines. Data from one well were used in this study to perform a seismic-to-well tie for seismic interpretation. The well contains check-shot data and is located near one of the 2D seismic lines (Fig. 2B).-The 2D seismic line passes through the well data with check-shot information. The 3D survey has 429 inlines and 554 crosslines, where these lines are oriented with NW-SE and NE-SW directions, respectively. The seismic cube extends down to a 3002-ms with a 4ms sampling interval and is prestack time-migrated. The 2D seismic lines were used in the lithostratigraphic interpretation to transfer the well-lithostratigraphic information (Açu Fm and basement tops) to the seismic cube area (Fig. 2).

3.2 Attributes analysis

To extract more information from the main reflectors, various attribute analyses have been performed (e.g., Chopra and Marfurt, 2007). Three main attributes have been applied: variance, cosine of phase, and dip illumination.

The variance attribute is a coherence attribute and is also considered a reverse version of semblance, which has been used in previous applications to indicate seismic breaks (Iacopini et al., 2012; Liao et al., 2019, 2020; Phillips et al., 2019; Oliveira et al., 2023). These attributes calculate the similarity of seismic waveforms between adjacent traces (time-lagged cross-correlation in both inline and crossline directions) by estimating the coherence coefficient (Chopra and Marfurt, 2007). Variance can therefore reveal differences between seismic traces

https://doi.org/10.5194/egusphere-2025-3487
Preprint. Discussion started: 16 September 2025

and transform a continuity volume into a discontinuity volume, highlighting structural and stratigraphic boundaries (Brown, 2004; Mituku and Omosanya, 2020).

The cosine of phase attribute (Taner et al., 1979) is derived from the instantaneous phase of the seismic signal and represents the cosine of the phase angle. Unlike amplitude, the cosine of phase is less sensitive to amplitude variations, rather emphasizing phase-related changes in the seismic signature. The present study utilizes this attribute to reveal the lateral continuity between hydrothermal vents and the surrounding layers. The literature has extensively discussed the use of this attribute in the exploration of subtle discontinuities and mapping reflector continuities (Barnes, 1996; Chopra and Marfurt, 2007), which has been applied to improve the interpretation of various geological features, such as channels (Sarhan and Safa, 2017).

We did use the dip illumination attribute (Wu and Chen, 2006), and this seismic attribute simulates an illumination pattern revealing dip structure in the timeslice and can highlight these dip differences, using shine or color variation effect on a seismic map. Dip illumination is often used to detect structural features such as faults, folds, and fractures in the rotated layers of seismic lines (Lisle, 1994; Hesthammer and Fossen, 1997). The attribute is very efficient on time slices, and geological features are revealed when this attribute defines a reflective surface on which a discontinuity measure is estimated (Chopra and Marfurt, 2007). We used the dip illumination attribute to support the location and mapping of each fluid pipe previously highlighted by the variance answer, which enhances the scatter and discontinuities. The fluid pipes were then extracted into bodies by isolating the variance answer, allowing the hydrothermal vents to be visualized in a 3D perspective.

3.3 Apparent Aspect Ratio (ARA)

We used the Apparent Aspect Ratio (ARA), which is a quantitative measure used to assess the plan-view geometry of fluid escape pipes identified in 3D seismic data (Maestrelli et al., 2017). It is defined as the ratio between the lengths of the long and short axes of a pipe's cross-section, measured along seismic inlines and crosslines. Since these directions may not align with the true maximum and minimum dimensions of the structure, the resulting value is only an approximation of the actual elongation. For this reason, it is referred to as "apparent" and cannot be directly used to infer regional stress orientations. Despite this limitation, the ARA is useful for distinguishing between circular and elongated pipe geometries. Values close to 1 indicate pipes with a nearly circular shape, while higher values suggest elliptical or more elongated forms in plan view. This distinction can provide important insights into the morphology and potential development mechanisms of these features.

To calculate the ARA, measurements are performed on cross-sections extracted from the seismic volume, typically at two different heights along the pipe: one near its base and another closer to its upper termination. The long and short axes are determined using orthogonal seismic slices—inline and crossline directions—intersecting the pipe at those levels. The ratio between these two axes yields the ARA value for that section. Pipes displaying highly irregular, coalescing, or interacting geometries are excluded from analysis due to the difficulty in defining consistent axis lengths along their conduit.

https://doi.org/10.5194/egusphere-2025-3487
Preprint. Discussion started: 16 September 2025

4. RESULTS

4.1 Mapping by conventional seismic interpretation

The study area comprises part of the onshore Potiguar Basin, featuring a post-rift seismic unit and basement rocks. Two lithostratigraphic formations (Açu and Jandaíra) are identified and described above the basement reflector (Fig. 3B). The basement exhibits discontinuous, scattered reflectors, with its top marked by green dots (Fig. 3b). This seismic facies is characterized by continuous reflectors often disrupted by mound-like or convex structures intruding the overlying unit, displaying strong amplitude anomalies. The Açu Fm, directly overlying the basement, shows a coherent, homogeneous reflection pattern intersected by straight columnar units (Fig. 4b) and diffuse structures with poorly defined boundaries (Fig. 4a). The Jandaíra Fm, above the Açu Fm, displays more continuous and homogeneous facies, interrupted by diffuse low-amplitude anomalies. These amplitude anomalies present patchy disruptions in both horizontal and vertical continuity. In seismic lines, these patches appear as intrusive facies with chaotic reflectors cutting across the primary layering.

https://doi.org/10.5194/egusphere-2025-3487
Preprint. Discussion started: 16 September 2025

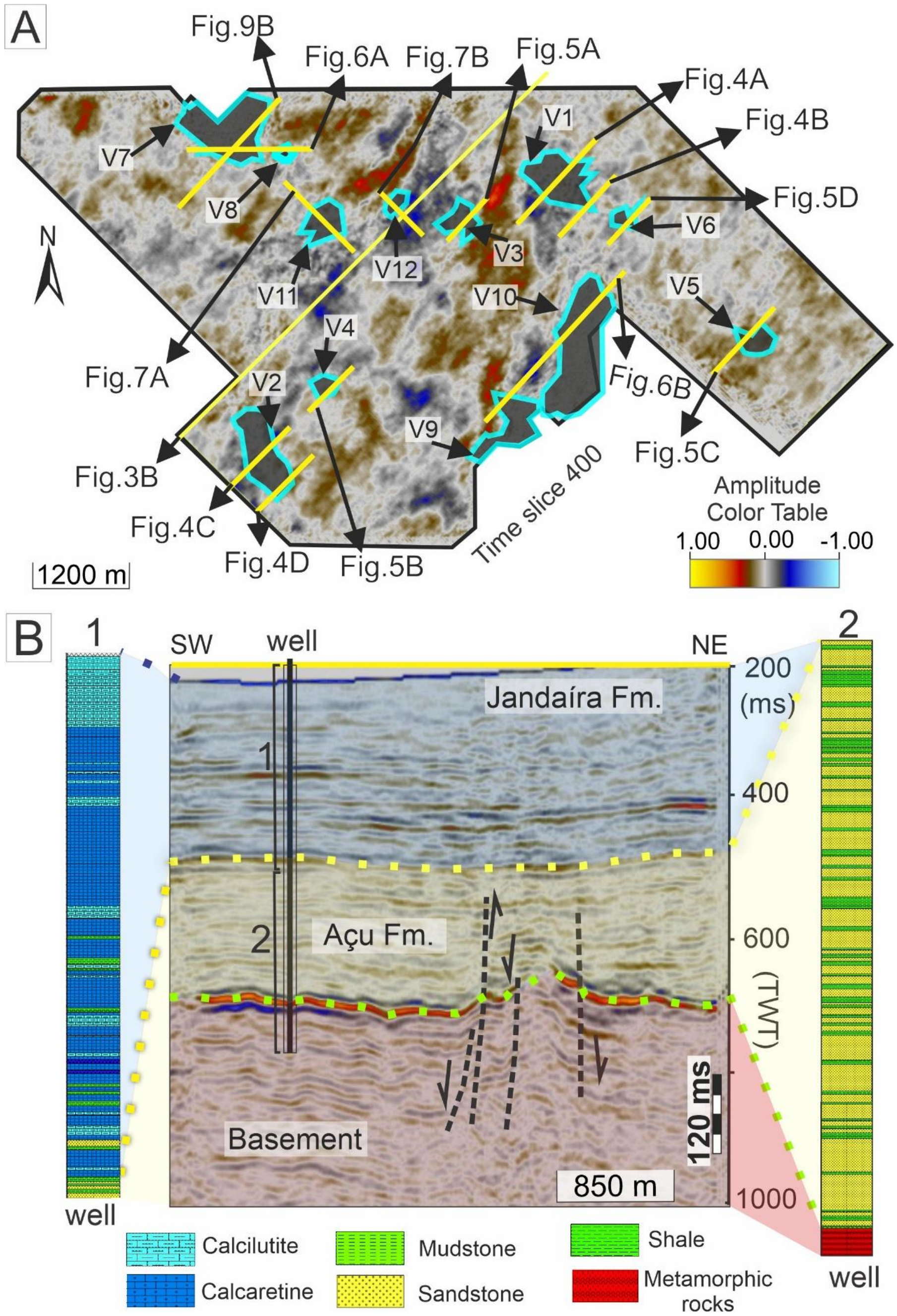

Figure 3 (A) Vents locations in the normal amplitude at the time slice -400ms. Blue shapes represent vents shapes. Yellow lines – seismic sections interpreted location in

this study. V - Vents . (B) Lithostratigraphic interpretation of a vertical section based on the well data. Vertical exaggeration: 5x.

The discontinuous basement reflectors suggest a highly fractured or heterogeneous igneous/metamorphic basement. The mound-like intrusions and amplitude anomalies may indicate igneous bodies or fluid migration pathways. The Açu Fm columnar and diffuse structures likely represent sedimentary deposits influenced by syn- or post-depositional intrusions. The chaotic patches in the Jandaíra Fm imply secondary processes such as fluid expulsion or soft-sediment deformation.

4.1.1 Characteristics of the hydrothermal vent complex

We characterized the main columnar vertical seismic facies intruding the main seismic package presenting deteriorated seismic signal, so the primary reflections either are absent or very weak (we will call thereafter those zones as wipe out zone, sensu Loseth et al., 2004) showing also edge discontinuities and attenuation of the reflectors (Figs. 4, 5, 6, and 7). Both along inlines or crosslines, some of these structures are represented by wipe out zones rimmed by an inner zone of high amplitude anomalies and an outer zone of dim amplitude anomalies. The various wipe out zones probably reflect various types of leakage processes through the low-permeable zone, contrasting with the surrounding reflector packages, where the disturbed zones stand out from the surrounding horizontal reflectors (Fig. 4a,b, and 6a,b). Therefore, other seismic sections show instead a more localized signal disturbance (Fig. 4c,d, and Fig. 5a,b), related to the leaking from fault structures. In Figures 7a and b, we observe a large disturbance zone broadening upward, making the signal interpretation near the surface difficult. Interestingly almost all figures show within all columnar areas of the disturbance

https://doi.org/10.5194/egusphere-2025-3487
Preprint. Discussion started: 16 September 2025

zone upward convex deflection of the main reflectors (Figs. 4, 5, 6, 7). This horizon deflection has been observed, except in some rare cases, with a different degree of development. In some of the largest examples with large wipe out zone, a chaotic expression of the seismic signal is visible: the reflection terminations of the deflected horizons show a clear loss of amplitude and a disruption of the internal architecture of the pipe.

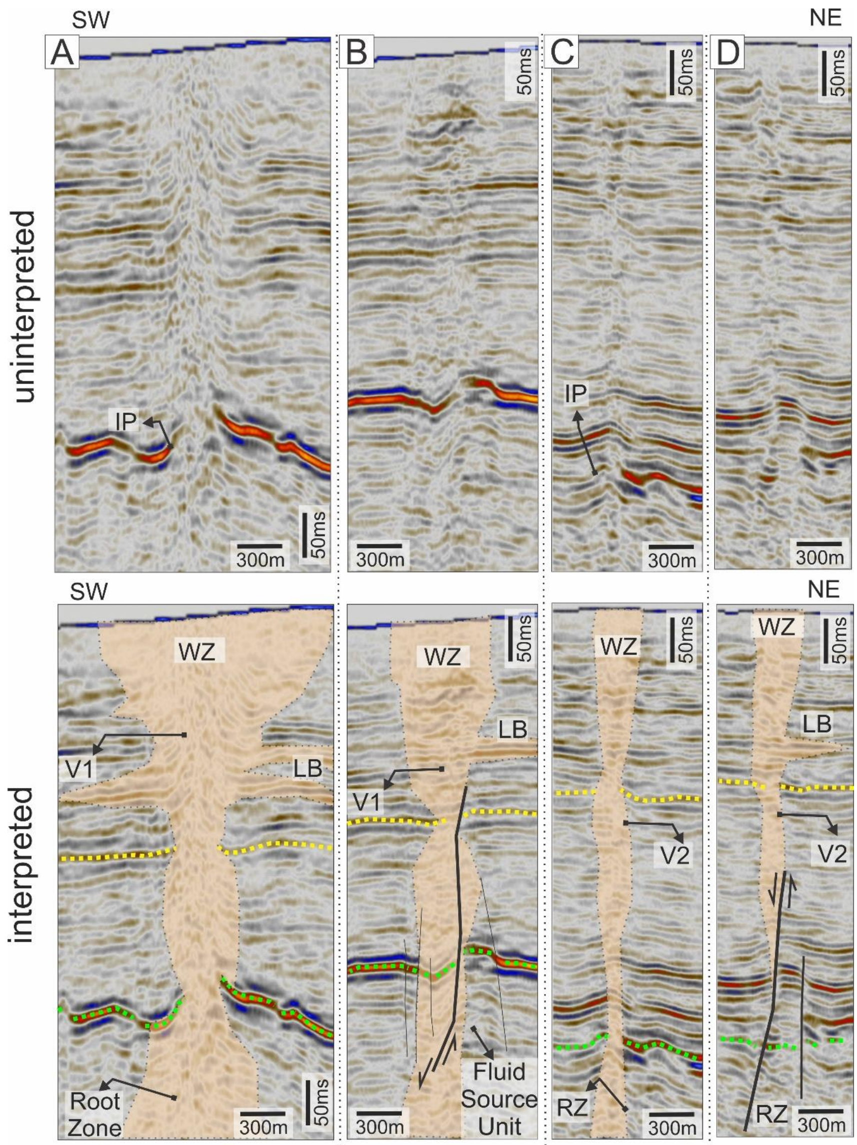

Figure 4 - Characterization of the vents 1 and 2 (V1 and V2) with their elements: Wipe out Zone (WZ), Dead Mixed Zone (DMZ), Inflection Point (IP), and Lateral Brightness (LB). When the vertical disturber zone is surrounded by bright reflectors, we refer to wipe out zone. Yellow dotted lines - Açu Fm top, green dotted lines - Basement top. Vertical exaggeration: 5x.

The root zone indicates the fluid source unit, which is below the basement top, and shows that those columnar wipe out zones are connected below the basement top. In the more localized condition the wipe out zone is exploiting

https://doi.org/10.5194/egusphere-2025-3487
Preprint. Discussion started: 16 September 2025

individual normal faults (Figs. 4, 5, 6, and 7). In our study case, all those columnar seismic facies are often connected to faults showing a normal fault kinematic.

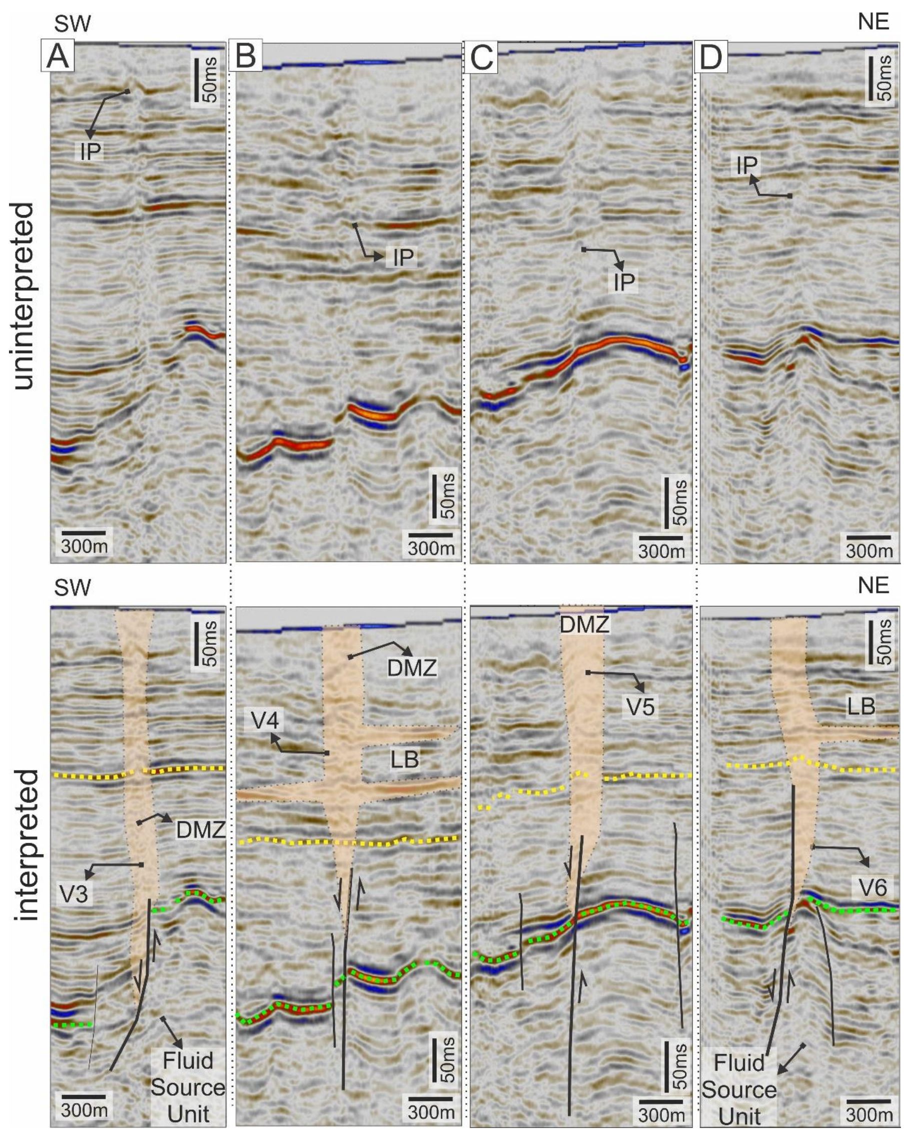

Figure 5 - Characterization of the vents (A) 3, (B) 4, (C) 5, and (D) 6 (V3, V4, V5, and V6) with their elements: Dead Mixed Zone (DMZ), Inflection Point (IP), and Lateral Brightness (LB). Yellow dotted lines - Açu Fm top, green dotted lines - Basement top. Vertical exaggeration: 5x.

https://doi.org/10.5194/egusphere-2025-3487
Preprint. Discussion started: 16 September 2025

Inside the main columnar wipe out zones, we can characterize some further seismic details (V1, V7, V10). The WZ, which are disturbed and chaotic zone, creates a zone of amplitude points or semi-continuous reflectors (Figs. 4, 6, and 7). The presence of inflection point (IP) of the seismic reflectors affecting the beddings, producing reflectors with dome-shaped, suggesting push-ups, which suggests a clear velocity changes in the seismic signal (Figs 4,5,6).

https://doi.org/10.5194/egusphere-2025-3487
Preprint. Discussion started: 16 September 2025

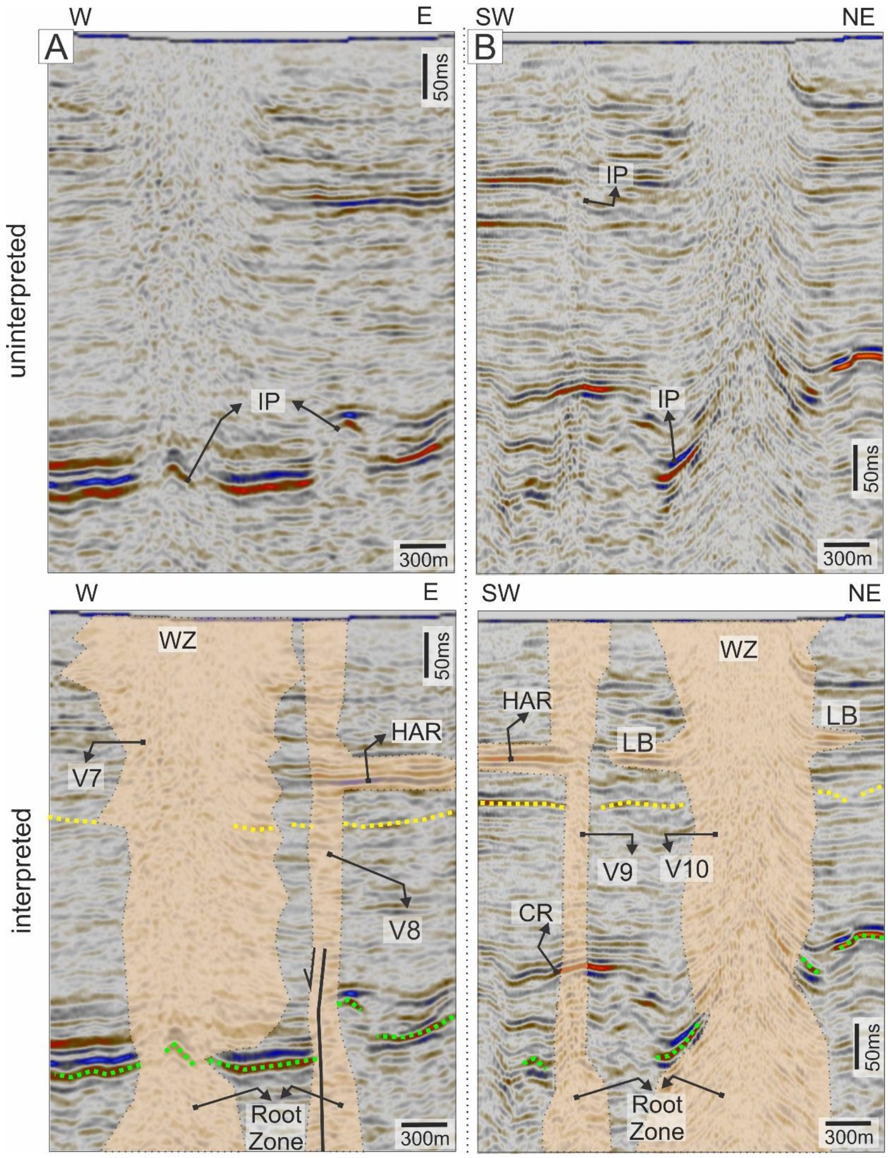

Figure 6 - Characterization of the (A) vents 7 and 8 (V7 and V8) and (B) vent 9 (V9) and 10 (V10) with their elements: Wipe out Zone (WZ), Inflection Point (IP), Lateral Brightness (LB), High Amplitude Reflectors (HAR), and Coherent Reflector (CR). Yellow dotted lines - Açu Fm top, green dotted lines - Basement top. Vertical exaggeration: 5x.

The columnar wipe out zones with a 'downward tapering cone' (V1, V7, and V10) increase their width through the top, crossing all the formations of the basin up to the surface (Figs 4, 5, and 6), making it impossible to characterize

https://doi.org/10.5194/egusphere-2025-3487
Preprint. Discussion started: 16 September 2025

the vents terminus in our study area. Close to all pipes, we do recognize high amplitude reflectors (HAR) and increasing their lateral brightness (LB) (Figs. 4, 5, 6, and 7).

https://doi.org/10.5194/egusphere-2025-3487
Preprint. Discussion started: 16 September 2025

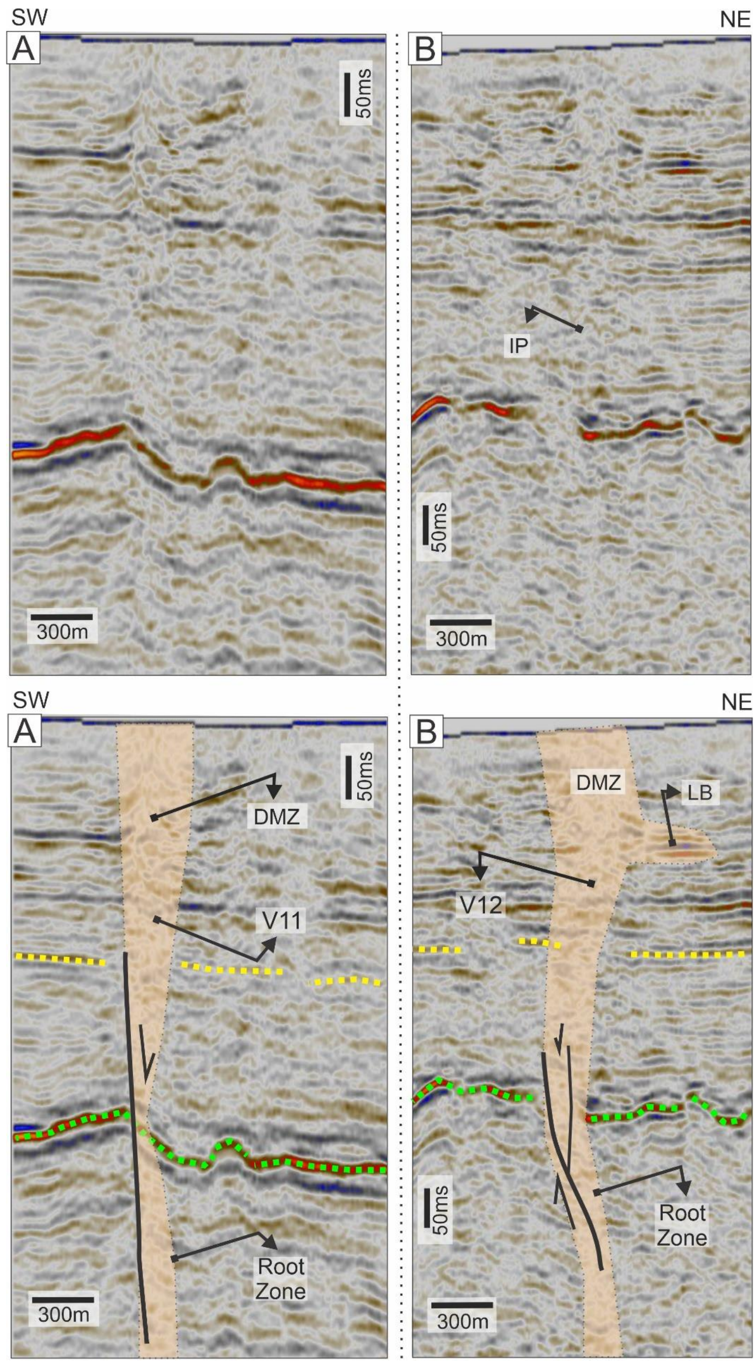

361

362 Figure 7 - Characterization of the fluid pipes 8 and 9 (P8 and P9) with their elements:
363 Dead Mixed Zone (DMZ), Inflection Point (IP), and Lateral Brightness (LB). Yellow dotted
364 lines - Açu Fm top, green dotted lines - Basement top. Vertical exaggeration: 5x.
365

https://doi.org/10.5194/egusphere-2025-3487
Preprint. Discussion started: 16 September 2025

4.2 Seismic Attributes

The application of seismic attributes such as dip illumination (Fig. 8B) and variance (Fig. 8C) confirms and enhances the signal anomalies corresponding to the wipe out zones, correlated to the vents, and to structures such as faults and fractures in their zones (Fig. 8D and E).

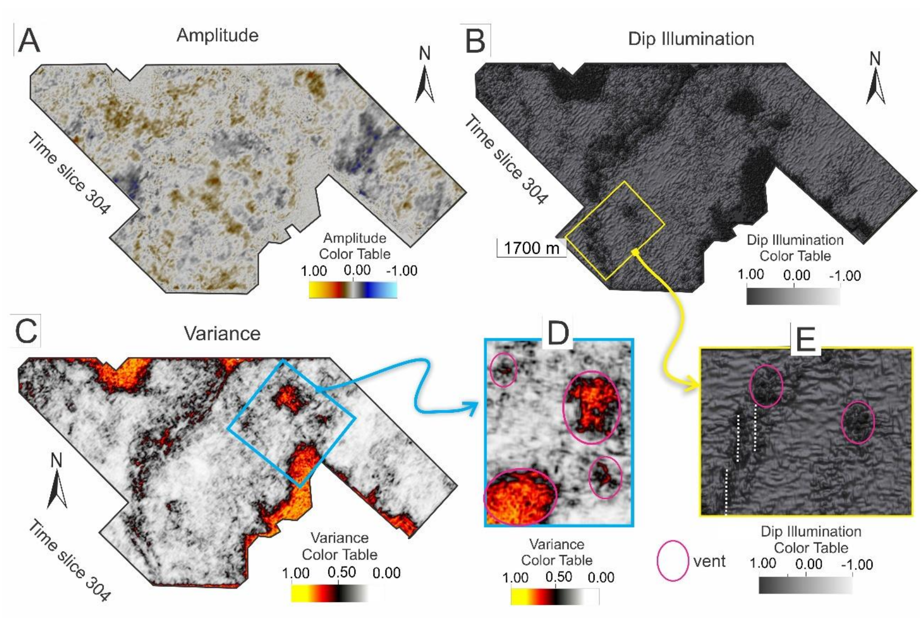

Figure 8 - Comparison of the seismic answers between (A) amplitude, (B) dip illumination, and (C) variance, revealing (D) the vents or fluid pipes and (E) the surrounding structures at the time slice 304ms. White dotted line – fault traces.

In vertical sections, the variance answer cover a large area of the wipe out zone related to the vent structures and cover entirely the dead mixed zones from the fluid pipes (Fig. 9). The variance attribute completely covers the fluid pipe shapes with low width variation (Fig. 9) and loses some areas for the vents with a conical shape (Fig. 9B). This correspondence between the variance attribute and the dead mixed zones provides an automatic vertical characterization of the pipes. The variance attribute reveals areas related to the

https://doi.org/10.5194/egusphere-2025-3487
Preprint. Discussion started: 16 September 2025

vents and fluid pipes, showing a great correspondence compared with the manual interpretation of the vents, which is observed by combining the variance answer with the normal amplitude for the pipes.

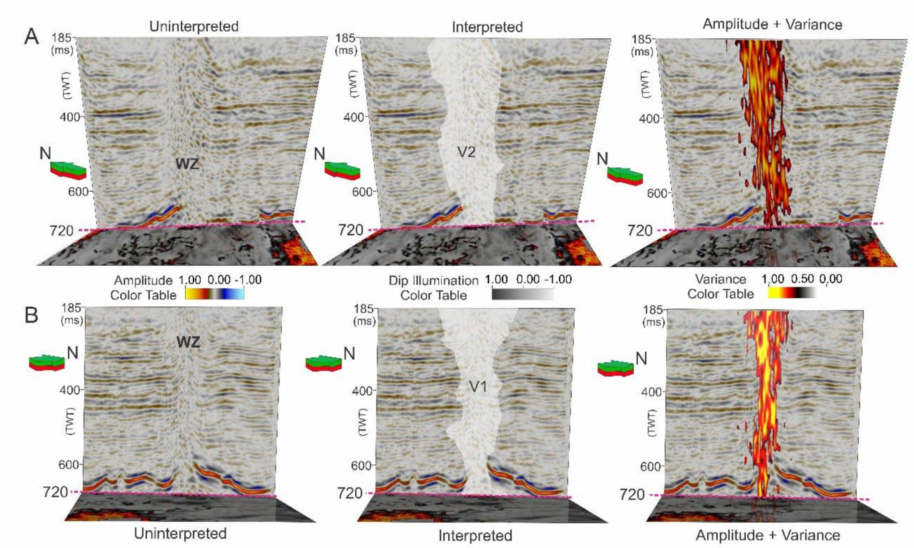

Figure 9 - External shape comparison between normal amplitude uninterpreted, interpreted, and variance attribute applied for the pipes V2 (A) and V1 (B). See Figure 3A for the location of the vents. Vertical exaggeration: 5x.

Even though applying the variance attribute is very effective in recognizing and characterizing hydrothermal vents, the vertical continuity of some fluid pipes can not be delimited (Fig. 10A and B). With the application of the cosine of phase attribute, the vertical and lateral continuity of the pipe anomalies caused by the seismic signal becomes more visible due to the contrast between the seismic facies pattern of the hydrothermal vents and the host rock. For some pipes, the shape of a ‘christmas tree’ becomes evident with the application of the cosine of phase (Fig. 10C), highlighting the variation in the lateral distribution of the fluid into the sedimentary formations.

https://doi.org/10.5194/egusphere-2025-3487
Preprint. Discussion started: 16 September 2025

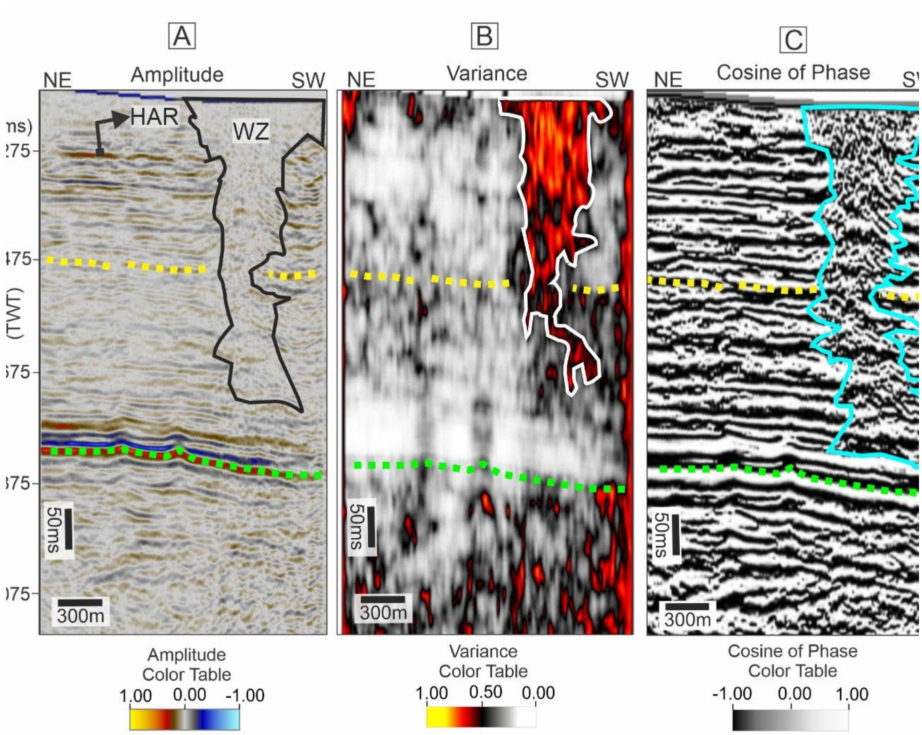

Figure 10 - Comparison of the pipe (V2) external shape between the normal amplitude (A), Variance (B), and Cosine of Phase (C) interpretation in a vertical section. See Figure 3A for the location of the vents. Vertical exaggeration: 5x.

Applying the cosine of phase attribute highlights the reflectors affected by the fluid, where the wipe out zone connect or penetrate the sedimentary formations of the basin (Fig. 11). The application of the cosine of phase attribute shows a new geometry of these structures, which are much more complex fluid bodies in a 3D perspective than previously highlighted by manual interpretations or compared to the variance attribute application.

https://doi.org/10.5194/egusphere-2025-3487
Preprint. Discussion started: 16 September 2025

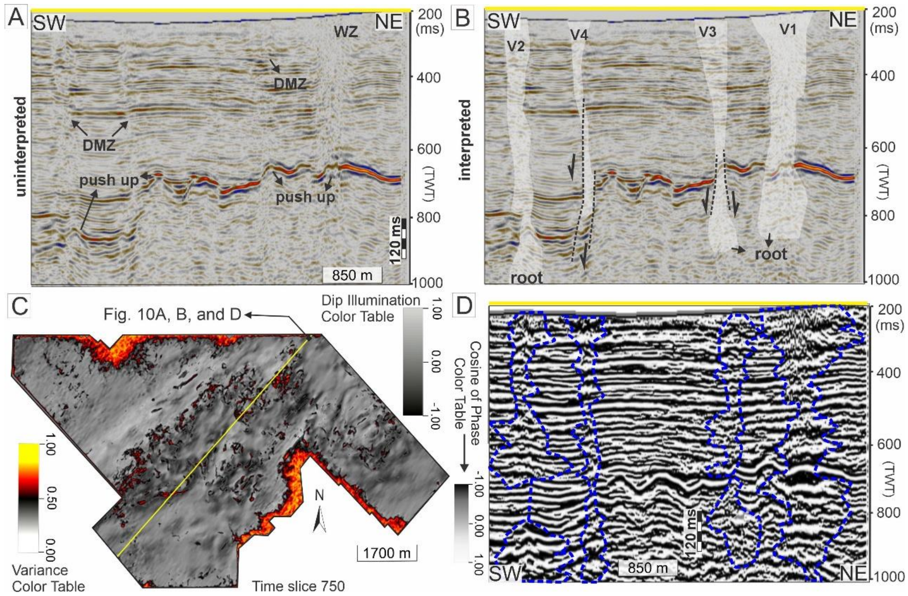

Figure 11 – Comparison between the fluid bodies geometry in (A) an uninterpreted vertical section, (B) with a manual interpretation of the vents and fluid pipes. (C) Time slice 750 ms applied Dip Illumination and Variance. (D) The cosine of phase attribute applied in the same seismic section. Vertical exaggeration: 5x.

4.3 Structural and geometric analysis of the wipe out zones

We chose two wipes out zones to analyze the geometric parameters of the external shape. The graph of the pipes' geometrical parameters consisted of the values of the wipe out zones axes 1 and 2, in the direction of the inlines and crosslines (Fig 12B), as well as the apparent aspect ratio by measuring the maximum and minimum fluid structures axes (Fig. 12C). All the values were measured at different depth levels from the fluid structures geobodies based on the variance attribute (Fig. 12A). We choose to show the values in a graphs with a fixed horizontal axis due the comparison between wipe out zones results.

The values measured above the inlines are higher for both fluid structures (V1 and V2), which are, therefore, more elongated in the NW-SE direction. For V1, the values of the axes in the inline and crossline directions are close to each

https://doi.org/10.5194/egusphere-2025-3487
Preprint. Discussion started: 16 September 2025

other (from 120m to 820m) in the inline direction, thus showing more dispersion of the data on the graph (Fig. 12B). The smaller axis of the V2 pipe is in the direction of the crossline (NE-SW) where its values vary from 120 to 450 m.

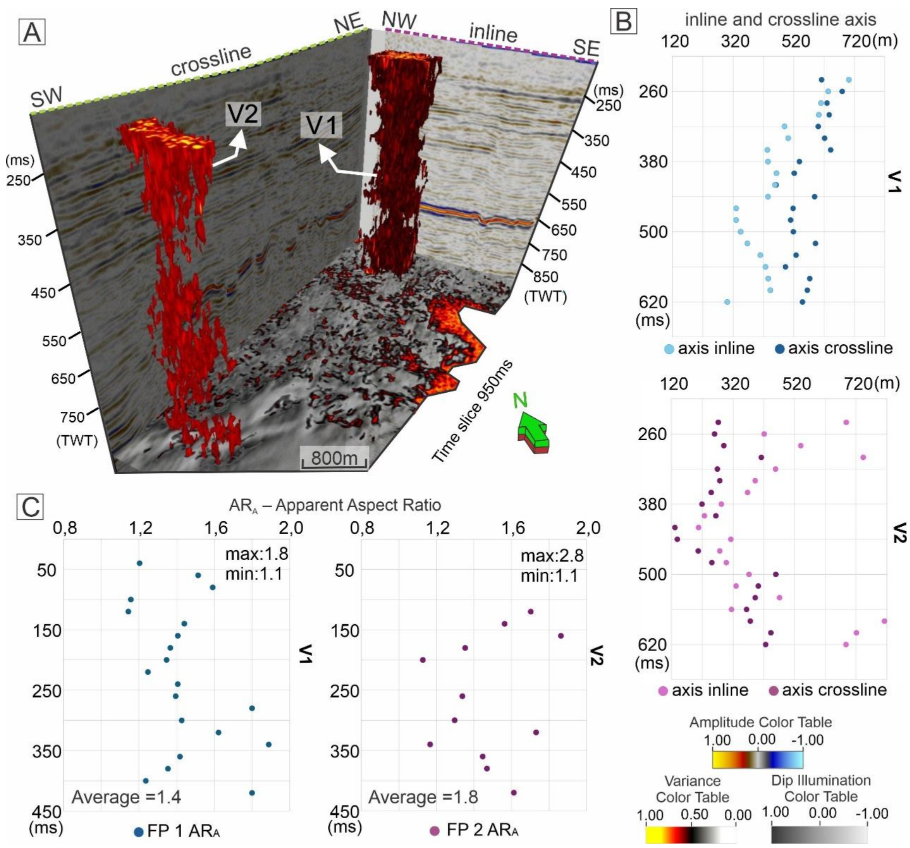

Figure 12 - (A) Geobodies of the vents 1 and 2 extracted based on the variance attribute. The graphs display the fluid pipe axis in inline and crossline directions (B) and their Apparent Aspect Ratio (ARA) to understand the fluid structures ellipticity in different levels. Vertical exaggeration: 5x.

We used the ARA to verify the ellipticity of the fluid structures. Based on Maestrelli et al. (2017), the apparent aspect ratio (ARA) was calculated as the ratio of the long axis to the short axis, approximating the pipe's elongation in plan view (circular if ARA ≈ 1, elliptical if ARA > 1). The values calculated from the maximum and minimum axes for the apparent aspect ratio exhibit greater

https://doi.org/10.5194/egusphere-2025-3487
Preprint. Discussion started: 16 September 2025

dispersion for the V2 pipe, with the opposite behavior observed in the V1 graph (Fig. 12C). The maximum radius values for V2 reach 2.8, which is 2 times the length of V1, with values of 1.8. This demonstrates a strongly elliptical classification of both pipes, with an AR_A average of 1.4 and 1.8 for V1 and V1, respectively. With this, the axis elongation striking to NW-SE for both pipes shows a greater directional control in the V2 values.

5. DISCUSSION

5.1 Geometry of the hydrothermal vents complex and fault systems

Previous studies associate hydrothermal vent complexes with faults, describing them as *pipe fault-related* (Planke et al., 2005) or fluid conduits (Magee et al., 2014; Rovere et al., 2014), often linked to structures above and around vents (Hansen, 2006; Kjoberg et al., 2017) or gas ascent within polygonal fault systems (Rovere et al., 2022). Our seismic analysis identifies "wipe-out zones" and "dead mixed zones" (Figs. 4–7), characterized by reflectors attenuation and internal chaotic pattern, and revealing that all analyzed pipes are associated with fault activity. This suggests their formation cannot be attributed solely to hydraulic fracturing or igneous intrusion-related pressure (Skogseid et al., 1992; Davies et al., 2002, 2012; Aarnes et al., 2010). Our description shows these vents are structurally controlled by regional faults, with root zones extending below the basement, indicating a fluid source within the crystalline basement. Surface studies by Menezes et al. (2019) corroborate this, showing the NW-SE Afonso Bezerra Fault System (active from rift to post-rift phases) cutting through the basin and basement. Seismic interpretation further reveals fluid conduits elongated along fault trends (Figs 12), with "inflection points" (IP)

https://doi.org/10.5194/egusphere-2025-3487
Preprint. Discussion started: 16 September 2025

forming dome-shaped geometries (Figs. 4–7), indicative of fluid ascent altering sedimentary layers. The internal signal and edge reflectors related to the vents show a push-up geometry, mostly dragging upward the main reflector (Figs. 4, 6, and 11), which suggests a denser intrusive unit, distinguishing it from a simple gas intrusion. Therefore, this is typical of hydrothermal rock or intrusion, which produces mineralization often re-fractured but the various intrusions. These conduits align with surface silicified breccias (Menezes et al., 2019), confirming their hydrothermal origin. Additionally, magmatic activity in the Potiguar Basin (e.g., Macau and Serra do Cuó events; Mizusaki et al., 2002; de Castro et al., 2012; Souza et al., 2019) likely contributed to thermal anomalies and sedimentary alteration, facilitating vent genesis.

The application of the cosine of phase attribute with the lateral brightness recognition (see LB in Figs. 4A, B, C, 5B, D, 6B, and 7B) reveals the vent fluids entering laterally in the sedimentary layers, changing the vents geometry (Fig. 13). The interaction between hydraulic fracturing, overpressure, and faults must be considered for a more comprehensive understanding of the genesis of the pipe systems, since structures as faults change the permeability influencing fluid flow (Caine et al., 1996; Faulkner et al., 2010; Palhano et al., 2023), acting as seals or conduits (Fisher et al., 1998; Bense et al., 2013; Torabi et la., 2021; Medici et al., 2021; Labry et al., 2025). Although previous studies suggest that hydraulic fracturing is a fundamental mechanism for the initiation and control of vent formation (Svensen et al., 2006; Alvarenga et al., 2016), we highlight that the development of brittle structures such as faults plays a crucial role in this process (Fig. 13). This implies that the evolution of the vents should be

https://doi.org/10.5194/egusphere-2025-3487
Preprint. Discussion started: 16 September 2025

interpreted in a broader tectonic context, where faults act as preferential pathways for fluid migration and control their ascent and escape.

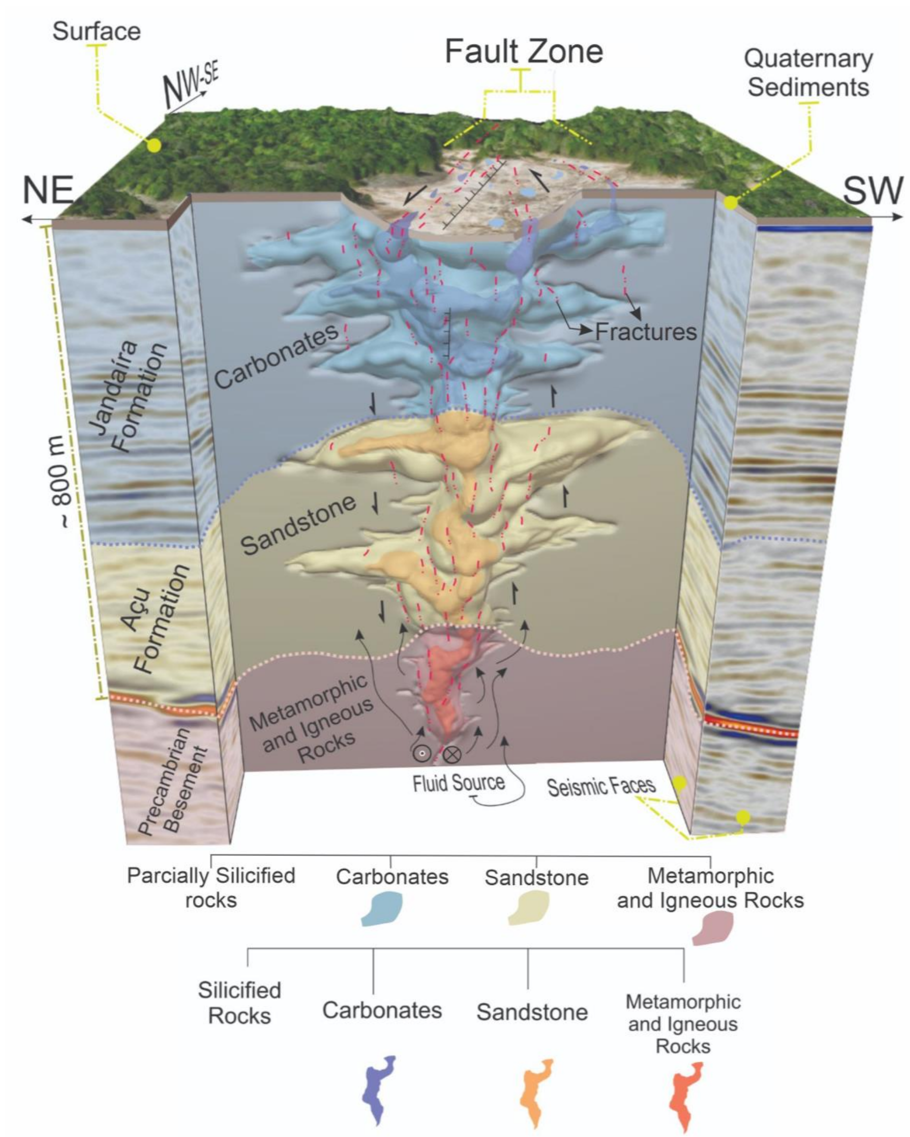

Figure 13 - The schematic model of fluid pipes ascending through the sedimentary basin controlled by a fault. Red traces - fractures.

Sedimentary basins that feature fluid pipes or hydrothermal vents, such as those in the Gulf of Mexico (Roberts and Carney, 1997; Aharon, 1994), the

https://doi.org/10.5194/egusphere-2025-3487
Preprint. Discussion started: 16 September 2025

North Sea (Cartwright et al., 2007; Løseth et al., 2009), the Santos Basin (Camboa and Rabinowitz, 1981; Mohriak et al., 2008), and the Campos Basin (Guardado et al., 1989; Bruhn and Walker, 2006), are characterized by dynamic geological systems where the circulation of thermal fluids plays a crucial role in rock modification and the generation of petroleum systems (Palhano et al., 2023; Maciel et al., 2024). In these basins, fluid pipes are often associated with tectonic and magmatic processes, creating migration pathways for hydrocarbons and contributing to the formation of structures such as sandstone dykes and hydrothermal alteration zones.

5.2 Seismic data limitation in the vents characterization

The hydrothermal vents are described in their parts as inner and outer zones based on the composition and structures of the vent outcropping, and how they affect the host rock (Jamtveit et al., 2004; Svensen et al., 2006). These vent zone descriptions allow the characterization of the fluid zones in terms of origin, host rock permeability, fluid pressure, and pipe complexity (Planke et al., 2005), where these zones were measured and analyzed using field data in previous studies. In the literature, major hydrothermal vent complex characterization has been conducted using seismic data by applying coherence attributes to reveal these structures (Svensen et al., 2003; Hansen, 2006; Kjoberg et al., 2017; Wang et al., 2019). In our case, we used seismic attributes such as variance, dip illumination, and cosine of phase to distinguish the disturbed zones from the fluid pipes and the host rock in the seismic data (Figs. 8, 9, 10, and 11), but even with this, it is impossible to define the internal vent zones as other previous studies (McDonnell et al., 2007; Magee et al., 2016; Mituku and Omosanya, 2020; Chen

https://doi.org/10.5194/egusphere-2025-3487
Preprint. Discussion started: 16 September 2025

et al., 2021). Therefore, the data resolution still limits the characterization of fluid pipe zones in the seismic data.

Coherence attributes alone can highlight other geological features besides faults (e.g., channel edges) or artifacts, and therefore need to be geologically validated. In our fluid pipes interpretation, it is evident that the fluid pipe detection in seismic data and the seismic attributes applied, such as variance and dip illumination, are particularly sensitive to these discontinuities (Figs. 8, 9, 10, and 11). We used seismic data from a shallow sedimentary package of the Potiguar Basin onshore portion, which presents noise or NR areas close to the surface or inside the basement, making the geometric characterization of the vents difficult. Among various seismic attributes, those that emphasize discontinuities between seismic reflectors or geological horizons are the most suitable ones for imaging faults (Chopra and Marfurt, 2005; Di et al., 2019; Libak et al., 2017; Oliveira et al., 2023) and vent complex areas as disturbed zones. However, the presence of noise poses a significant challenge and is very impacted to noise and no disturbance of the reflectors, as it can adversely affect the accuracy and reliability of seismic attribute results (Cohen et al., 2006; Hale, 2013; Wu et al., 2019).

6. CONCLUSIONS

Our results demonstrate that hydrothermal vent development in the Potiguar Basin is fundamentally controlled by fault activity, particularly the Afonso Bezerra Fault System. The strongly elliptical and elongated vent geometries aligned with fault trends contribute to the previous models that attribute vent formation solely to hydraulic fracturing from igneous intrusions. Instead, we propose a hybrid model where faults act to guide the fluid pathways, modify

https://doi.org/10.5194/egusphere-2025-3487
Preprint. Discussion started: 16 September 2025

permeability, and change the vent morphology. Fault zones not only localize vents but also enhance reservoir-scale permeability, with implications for hydrocarbon migration and hydrothermal mineralization.

The association of vents with regional fault systems suggests their formation is intrinsically linked to the basin's rift-related tectonic framework. This aligns with global analogs (e.g., Gulf of Mexico, North Sea), where vents develop along fault zones in magmatically active basins. The Potiguar Basin's silicified breccias and magmatic events (e.g., Macau and Serra do Cuó) further support a tectonic-magmatic interplay in the vent development.

While seismic attributes (variance, dip illumination, and cosine of phase) effectively delineate vent boundaries and disturbed zones, they cannot resolve internal vent zonation (e.g., inner/outer zones) observed in the field studies. Discontinuity-based attributes (e.g., coherence) are sensitive to vent structures but require geological validation to distinguish vents from other features. Variance and dip illumination proved most robust for mapping fault-vent relationships, though noise in shallow sedimentary sections limits geometric precision. Data resolution and near-surface noise remain key challenges, emphasizing the need for integrated approaches combining seismic, well, and outcrop data.

Author Contribution

L. S. B.O.: Conceptualization; Investigation; Methodology; Validation; Visualization; Roles/Writing - original draft; and Writing - review & editing

L.C.V.L.: Conceptualization; Investigation; Methodology; Visualization; Roles/Writing - original draft; and Writing - review & editing

D.I.: Conceptualization Investigation; Methodology; Formal analysis; Validation; Visualization; Roles/Writing - original draft; and Writing - review & editing

F. B.: Conceptualization; Investigation; Methodology; Supervision; Validation; Visualization; Roles/Writing - original draft; and Writing - review & editing

https://doi.org/10.5194/egusphere-2025-3487
Preprint. Discussion started: 16 September 2025

A. T.: Conceptualization; Formal analysis; Investigation; Methodology; Supervision; Validation; Visualization; Roles/Writing - original draft; and Writing - review & editing

B. A.: Conceptualization; Formal analysis; Investigation; Methodology; Supervision; Validation; Visualization; Writing - review & editing

J.F. de S.N.: Investigation; Methodology; Validation; Visualization;

P. E. F. M.: Visualization; Writing - review & editing

D. L. V.: Writing - review & editing;

V. La B.: Writing - review & editing;

F. H. R. B.: Conceptualization; Investigation; Methodology; Resources; Project administration; Supervision; Validation; Visualization; Roles/Writing - original draft; and Writing - review & editing.

The authors declare that they have no conflict of interest

ACKNOWLEDGES

This research was carried out in association with the ongoing R&D project registered as ANP 23505-1, "Processos e Caracterização de Rotas de Fluxo de Fluidos em Reservatórios Carstificados, Fraturados e Silicificados do Pré-Sal – Porocarste Fase II" (UFRN/UNB/UFPE/UFC/UFRA/IFRN/IFPB/Shell Brasil/ANP) – Porokarst Phase II – Processes and Characterization of fluid pathways in Karstified, Fractured and Silicified Reservoirs of the Presalt, sponsored by Shell Brasil under the ANP R&D levy. DLV thanks CNPq for its productivity grant (PQ grant).

REFERENCES

Aarnes, I., Svensen, H., Connolly, J.A., Podladchikov, Y.Y., 2010. How contact metamorphism can trigger global climate changes: Modeling gas generation around igneous sills in sedimentary basins. Geochim. Cosmochim. Acta 74 (24), 7179–7195. https://doi.org/10.1016/j.gca.2010.09.011.

https://doi.org/10.5194/egusphere-2025-3487
Preprint. Discussion started: 16 September 2025

Aharon, P., 1994. Geology and biology of modern and ancient submarine hydrocarbon seeps and vents: An introduction. *Geo-Marine Letters*, 14(2-3), 69-73. DOI: 10.1007/BF01203716.

Alvarenga, R.S., Iacopini, D., Kuchle, J., Scherer, C.M.S., Goldberg, K., 2016. Seismic characteristics and distribution of hydrothermal vent complexes in the cretaceous offshore rift section of the Campos Basin, offshore Brazil. Mar. Pet. Geol. 74, 12–25. https://doi.org/10.1016/j.marpetgeo.2016.03.030.

Araripe, P.T., Feijó, F.J., 1994. Bacia Potiguar. Boletim de Geociências da Petrobras 8 (1), 127e141.

Bahorich, M. S., Farmer, S. L., 1995. 3-D seismic discontinuity for faults and stratigraphic features: The coherence cube; SEG Technical Program Expanded Abstracts: 93-96. https://doi.org/10.1190/1.1887523.

Barnes, A. E., 1996. Theory of 2-D complex seismic trace analysis. Geophysics, 61(1), 264-272. https://doi.org/10.1190/1.1443947.

Bense, V. F., Gleeson, T., Loveless, S. E., Bour, O., & Scibek, J. (2013). Fault zone hydrogeology. Earth-Science Reviews, 127, 171-192. https://doi.org/10.1016/j.earscirev.2013.09.008.

Bertani, R.T., Costa, I.G., Matos, R.M.D., 1990. Evolução tectono-sedimentar, estilo estrutural e habitat do petróleo na Bacia Potiguar. In: Gabaglia, G.P.R., Milani, E.J. (Eds.), Origem e evolução de Bacias Sedimentares. Petrobras, Rio de Janeiro, pp. 291-310.

Bezerra, F. H. R., Amaral, R. F., Silva, F. O., Sousa, M. O. L., Vieira, M. M., Lima, E. N. M., Aquino, M. R., Fonseca, V. P., 2009. Nota explicativa da folha Macau, SB.24-X-D-II. CPRM, https://rigeo.sgb.gov.br/handle/doc/18284.

https://doi.org/10.5194/egusphere-2025-3487
Preprint. Discussion started: 16 September 2025

Bruhn, C. H. L., & Walker, R. G., 1997. Internal architecture and sedimentary evolution of coarse-grained, turbidite channel-levee complexes, Early Eocene Regência Member, Campos Basin, Brazil. *Sedimentology*, 44(1), 17-46. https://doi.org/10.1111/j.1365-3091.1997.tb00422.x.

Caine, J. S., Evans, J. P., & Forster, C. B., 1996. Fault zone architecture and permeability structure. Geology, 24(11), 1025-1028.

Camboa, L., & Rabinowitz, P. D., 1981. The Rio Grande Rise and the Brazil Basin: Geological and geophysical studies. *Deep Sea Research Part A. Oceanographic Research Papers*, 28(9), 873-891.

Cartwright, J., Huuse, M., & Aplin, A., 2007. Seal bypass systems. *AAPG Bulletin*, 91(8), 1141-1166.

Cartwright, J., Santamarina, C., 2015. Seismic characteristics of fluid escape pipes in sedimentary basins: Implications for pipe genesis. Mar. Pet. Geol. 65, 126–140. https://doi.org/10.1016/j.marpetgeo.2015.03.023.

Chen, D., Zhang, G., Wang, X., Wang, Z., Chen, S., Dong, D., 2021. Seismic features and origin of fluid escape pipes offshore Hainan Island on the northern slope of South China Sea, Marine and Petroleum Geology, V. 133, 105276, ISSN 0264-8172, https://doi.org/10.1016/j.marpetgeo.2021.105276.

Chopra, S., and K. J. Marfurt, 2005, Seismic attributes: A historical perspective: Geophysics, 70, no. 5, 3SO–28SO, doi: 10.1190/1.2098670.

Chopra, S., and K. J. Marfurt, 2007, Volumetric curvature attributes for fault/fracture characterization: First Break, 25, 19–30, doi: 10.3997/1365-2397.2007019.

https://doi.org/10.5194/egusphere-2025-3487
Preprint. Discussion started: 16 September 2025

Cohen, I., N. Coult, and A. A. Vassilou, 2006, Detection and extraction of fault surfaces in 3D seismic data: Geophysics, 71, no. 4, P21–P27, doi: 10.1190/1.2215357.

Davies, R., Bell, B.R., Cartwright, J.A., Shoulders, S., 2002. Three-dimensional seismic imaging of Paleogene dike-fed submarine volcanoes from the Northeast Atlantic margin. Geology 30 (3), 223–226. https://doi.org/10.1130/0091-7613(2002)030<0223:TDSIOP>2.0.CO;2.

Davies, R. J., Mathias, S. A., Moss, J., Hustoff, S., Newport, L., 2012. Hydraulic fractures: How far can they go?. Marine and Petroleum Geology, V 37, Issue 1, P 1-6, ISSN 0264-8172, https://doi.org/10.1016/j.marpetgeo.2012.04.001.

de Castro, D. L., 2011. Gravity and magnetic joint modeling of the Potiguar Rift Basin (NE Brazil): Basement control during Neocomian extension and deformation. Journal of South American Earth Sciences, 31, 186-198. doi:10.1016/j.jsames.2011.01.005.

de Castro, D. L., Bezerra, F. H. R., Sousa, M. O. L., & Fuck, R. A., 2012. Influence of Neoproterozoic tectonic fabric on the origin of the Potiguar Basin, northeastern Brazil and its links with West Africa based on gravity and magnetic data. *Journal of Geodynamics*, 54, 29-42. https://doi.org/10.1016/j.jog.2011.09.002.

de Castro, D.L., Reis Jr., J.A., Teixeira, W.L.E., Silva, V.A., Lima Filho, F.P., 2014. GPR Imaging Techniques Applied in 3D environment: example in inactive dunes. Revista Brasileira de Geofísica 32, 273–289. http://dx.doi.org/10.22564/rbgf.v32i2.482.

de Castro, D. L. and Bezerra, F. H. R.: Fault evolution in the Potiguar rift termination, equatorial margin of Brazil, Solid Earth, 6, 185–196, https://doi.org/10.5194/se-6-185-2015, 2015.

Delaney, J. R., Robigou, V., McDuff, R. E., 1992. Geology of a Vigorous Hydrotherma System on the Endeavour Segment, Juan de Fuca Ridge. Journal of Geophysical Research, V 97. https://doi.org/10.1029/92JB00174.

Mahiques, M. M., Schattner, U., Lazar, M., Sumida, P. Y. G., Souza, L. A. P. D., 2017. An Extensive Pockmark Field on the Upper Atlantic Margin of Southeast Brazil: Spatial Analysis and its Relationship with Salt Diapirism. Heliyon 3, e00257. doi:10.1016/j.heliyon.2017.e00257.

Di, H., M. A. Shafiq, Z. Wang, and G. AlRegib, 2019, Improving seismic fault detection by super-attribute-based classification: Interpretation, 7, no. 3, SE251–SE267, doi: 10.1190/INT-2018-0188.1.

Faulkner, D.R., Jackson, C.A.L., Lunn, R.J., Schlische, R.W., Shipton, Z.K., Wibberley, C.A.J., Withjack, M.O., 2010. A review of recent developments concerning the structure, mechanics and fluid flow properties of fault zones: Journal of Structural Geology, 32,1557-1575. https://doi.org/10.1016/j.jsg.2010.06.009.

Finn, C. A., Bedrosian, P. A., Holbrook, W. S., Bloss, B. R., Crosble, J., 2022. Geophysical imaging of the Yellowstone hydrothermal plumbing system, Nature, V. 603, https://doi.org/10.1038/s41586-021-04379-1.

Fonseca, J. C., Ranero, C. R., Vannucchi, P., Iacopini, D., & Vital, H., 2024. The tectonic structure and evolution of the Potiguar-Ceará rifted margin of Brazil. Tectonics, 43, e2023TC008184. https://doi.org/10.1029/2023TC008184

Françolin, J. B. L., Cobbold, P. R., Szatmari, P., 1994, Faulting in the early Cretaceous Rio do Peixe basin (NE Brazil) and its significance for the opening of the Atlantic: Journal of Structural Geology, 16, 647-661; doi: 10.1016/0191-8141(94)90116-3.

https://doi.org/10.5194/egusphere-2025-3487
Preprint. Discussion started: 16 September 2025

Guardado, L. R., Camboa, L. A. P., & Lucchesi, C. F., 1990. Petroleum geology of the Campos Basin, Brazil, a model for a producing Atlantic type basin. *AAPG Memoir*, 48, 3-79.

Hale, D., 2013, Methods to compute fault images, extract fault surfaces, and estimate fault throws from 3D seismic images: Geophysics, 78, no. 2, O33–O43, doi: 10.1190/geo2012-0331.1.

Hansen, D.M., 2006. The morphology of intrusion-related vent structures and their implications for constraining the timing of intrusive events along the NE Atlantic margin. Journal of Geological Society 163 (5), 789–800. https://doi.org/10.1144/0016-76492004-167.

Hansen, D.M., Cartwright, J., 2006. The three-dimensional geometry and growth of forced folds above saucer-shaped igneous sills. Journal of Structural Geology 28, 1520-1535. doi:10.1016/j.jsg.2006.04.004.

Hansen, D.M., Redfern, J., Federici, F., Di Biase, D., Bertozzi, G., 2008. Miocene igneous activity in the Northern Subbasin, offshore Senegal, NW Africa. Marine and Petroleum Geology. 25, 1e15.

Hesthammer, J., Fossen, H., 1997. Research article: The influence of seismic noise in structural interpretation of seismic attribute maps. First Break, 15. https://doi.org/10.3997/1365-2397.1997007.

Iacopini, D., Butler, R. W. H., & Purves, S. (2012). Seismic imaging of thrust faults and structural damage: A visualization workflow for deepwater thrust belts. First Break, 30(5), 39–46. https://doi.org/10.3997/1365-2397.30.5.58681

Jackson, C. A-L., Schofield, N., Golenkov, B., 2013. Geometry and controls on the development of igneous sill-related forced folds: A 2-D seismic reflection case study from offshore southern Australia. Geological Society of America Bulletin 2013;125, no. 11-12;1874-1890. doi: 10.1130/B30833.1.

Jamtveit, B., Svensen, H., Podladchikov, Y.Y., Planke, S., 2004. Hydrothermal vent complexes associated with sill intrusions in sedimentary basins. Phys. Geol. High-Level Magmatic Syst. Geol. Soc. Lond., Spec. Publ. 234, 233–241. https://doi.org/10.1144/GSL.SP.2004.234.01.15.

Kennish, M.J., Lutz, R.A., Simoneit, B.R.T., 1992. Hydrothermal activity and petroleum generation in the Guaymas Basin. Reviews in Aquatic Sciences 6, 467–477.

Kjoberg, S., Schmiedel, T., Planke, S., Svensen, H.H., Millett, J.M., Jerram, D.A., Galland, O., Lecomte, I., Schofield, N., Haug, O.T., Helsem, A., 2017. 3D structure and formation of hydrothermal vent complexes at the Paleocene-Eocene transition, the More Basin, mid-Norwegian margin. Interpretation 5 (3), SK65-SK81. https:// doi.org/10.1190/INT-2016-0159.1.

Labry, C., Funedda, A., Torabi, A., Arras, C., Da Pelo,S., 2025. Deformation style and fluid flow behaviour in a faulted siliciclastic-carbonate sequence. Journal of Structural Geology, V 199, 105468. https://doi.org/10.1016/j.jsg.2025.105468.

Liao, Z., H. Liu, B. M. Carpenter, K. J. Marfurt, and Z. Reches, 2019, Analysis of fault damage zones using three-dimensional seismic coherence in the Anadarko Basin, Oklahoma: AAPG Bulletin, 103, 1771–1785, doi: 10.1306/1219181413417207.

Liao, Z., L. Hu, X. Huang, B. M. Carpenter, K. J. Marfurt, S. Vasileva, and Y. Zhou, 2020, Characterizing damage zones of normal faults using seismic variance in the Wangxuzhuang oilfield, China: Interpretation, 8, no. 4, SP53–SP60, doi: 10.1190/INT-2020-0004.1.

Libak, A., Alaei, B., Torabi, A., 2017. Fault visualization and identification in fault seismic attribute volumes: Implications for fault geometric characterization. Interpretation, 5 (2), pp. B1-B16, doi:10.1190/INT-2016-0152.1

Lisle, R. J., 1994. Detection of Zones of Abnormal Strains in Structures Using Gaussian Curvature Analysis. American Association of Petroleum Geologists, 78.

Løseth, H., Gading, M., & Wensaas, L., 2009. Hydrocarbon leakage interpreted on seismic data. *Marine and Petroleum Geology*, 26(7), 1304-1319. https://doi.org/10.1016/j.marpetgeo.2010.10.001.

Maciel, I. B., Balsamo, F., Bezerra, F.H.R., Nogueira, F.C.C., Berio, L. R., Brod, J.A., Souza, Z. S., Matos-Pimentel, H.L.S., Carvalho, B.R.B.M., Souza, J.A.B., 2024. Hydrothermal silicification along rift border faults in the Rio do Peixe basin, Brazil. Marine and Petroleum Geology, Volume 168, 107025, ISSN 0264-8172, https://doi.org/10.1016/j.marpetgeo.2024.107025.

Maestrelli, D., Iacopini, D., Jihad, A.A., Bond, C.E., Bonini, M., 2017. Seismic and structural characterization of fluid escape pipes using 3D and partial stack seismic from the Loyal Field (Scotland, UK): a multiphase and repeated intrusive mechanism. Marine and Petroleum Geology, 88, 489–510. https://doi.org/10.1016/j.marpetgeo.2017.08.016.

Magee, C., Jackson, C.L., Schofield, N., 2014. Diachronous sub-volcanic intrusion along deep-water margins: Insights from the Irish Rockall Basin. Basin Res. 26 (1), 85–105. https://doi.org/10.1111/bre.12044.

Magee, C., Duffy, O. B., Purnell, K., Bell, R. E., Jackson, C.L., Reeve, M. T., 2016. Fault-controlled fluid flow inferred from hydrothermal vents imaged in 3D seismic reflection data, offshore NW Australia. Basin Research, 28, 299–318, doi: 10.1111/bre.12111.

https://doi.org/10.5194/egusphere-2025-3487
Preprint. Discussion started: 16 September 2025

Matos, R.M.D., 1992. The northeast Brazilian rift system. Tectonics 11 (4), 766e791.

Matos, R.M.D., 1999. History of the Northeast Brazilian Rift System: Kinematic Implications for the Breakup between Brazil and West Africa. In: Cameron, N.R., Bate, R.H., Clure, V.S. (Eds.), The Oil and Gas Habitats of the South.

McDonell, A., Loucks, R. G., Dooley, T., 2007. Quantifying the origin and geometry of circular sag structures in northern Fort Worth Basin, Texas: Paleocave collapse, pull-apart fault systems, or hydrothermal alteration?; The American Association of Petroleum Geologists, DOI:10.1306/05170706086.

Atlantic. Special Publication, vol. 153. Geological Society, London, pp. 55e73.

Menezes, C. P., Bezerra, F. H. R., Balsamo, F., Mozafari, M., Vieira, M. M., Srivastava, N. K., & de Castro, D. L. (2019. Hydrothermal silicification along faults affecting carbonate- sandstone units and its impact on reservoir quality, Potiguar Basin, Brazil. Marine and Petroleum Geology, 110, 198–217. https://doi.org/10.1016/j.marpetgeo.2019.07.018

Mizusaki, A. M. P., Thomaz Filho, A., & Milani, E. J., 2002. Mesozoic and Cenozoic igneous activity and its tectonic control in northeastern Brazil. *Journal of South American Earth Sciences*, 15(2), 183-198. https://doi.org/10.1016/S0895-9811(02)00014-7.

Mituku, S. B., Omosanya, K. O., 2020. Morphometric scaling of subsurface vent complexes: implications for a new classification scheme. Geo-Marine Letters, 40:659–674. https://doi.org/10.1007/s00367-020-00661-9.

Mohriak, W. U., Nemčok, M., & Enciso, G., 2008. South Atlantic divergent margin evolution: rift-border uplift and salt tectonics. *Geological Society, London, Special Publications*, 294(1), 365-398.

https://doi.org/10.5194/egusphere-2025-3487
Preprint. Discussion started: 16 September 2025

Moss, J. L., & Cartwright, J., 2010. 3D seismic expression of km-scale fluid escape pipes from offshore Namibia. Basin Research, 22(4), 481-501. https://doi.org/10.1111/j.1365- 2117.2010.00461.x

Oliveira, L. S. B., Alaei, B., Torabi., A., Leopoldino-Oliveira, K. M., Vasconcelos, D. L., Bezerra, F. H. R., Nogueira, F. C. C., 2023. Automatic 3D fault detection and characterization — A comparison between seismic attribute methods and deep learning," Interpretation 11: T793-T808. Htt.ps://doi.org/10.1190/INT-2023-0016.1.

Omosanya, K.O., Eruteya, O.E., Siregar, E.S., Zieba, K.J., Johansen, S.E., Alves, T.M., Waldmann, N.D., 2018. Three-dimensional (3-D) seismic imaging of conduits and radial faults associated with hydrothermal vent complexes (Voring Basin, Offshore Norway). Marine and Petroleum Geology. 399, 115–134. https://doi.org/10.1016/j.margeo.2018.02.007.

Roberts, H. H., & Carney, R. S., 1997. Evidence of episodic fluid, gas, and sediment venting on the northern Gulf of Mexico continental slope. *Economic Geology*, 92(7-8), 863-879.

Rovere, M., Gamberi, F., Mercorella, A., Rashed, H., Gallerani, A., Leidi, E., Marani, M., Funari, V., Pini G. A., 2014. Venting and seepage systems associated with mud volcanoes and mud diapirs in the southern Tyrrhenian Sea. Marine Geology, 347, 153–171. http://dx.doi.org/10.1016/j.margeo.2013.11.013.

Rovere, M., Mercorella, A., Gamberi, F., Zgur, F., 2022. Hydrothermal Vent Complexes Control Seepage and Hydrocarbon Release on the Overriding Plate of the Tyrrhenian-Ionian Subduction System (Paola Basin), Frontier Earth Science. 10:852786. doi: 10.3389/feart.2022.852786.

https://doi.org/10.5194/egusphere-2025-3487
Preprint. Discussion started: 16 September 2025

Palhano, L. C., Nogueira, F.C.C., Marques, F. O., Vasconcelos, D.L. Bezerra, F. H. R., Souza, J.A.B., Nicchio, M. A., Perez, Y. A. R., Balsamo, F., 2023. Influence of hydrothermal silicification on the physical properties of a basin-boundary fault affecting arkosic porous sandstones, Rio do Peixe Basin, Brazil. Marine and Petroleum Geology, V148, 106062, ISSN 0264-8172, https://doi.org/10.1016/j.marpetgeo.2022.106062.

Pessoa Neto, O. C., Soares, U. M., Silva, J. G. F., Roesner, E. H., Florencio, C. P., & Souza, C. A. V., 2007. Bacia Potiguar. Boletim de Geociências da Petrobras, 15(2), 357-369. https://bgp.petrobras.com.br/bgp/article/view/326.

Phillips, T. B., C. A.-L. Jackson, R. E. Bell, and A. A. Valencia, 2019, Rivers, reefs, and deltas: Geomorphological evolution of the Jurassic of the Farsund Basin, offshore southern Norway: Petroleum Geoscience, 26, 81–100, doi: 10.1144/petgeo2018-056.

Planke, S., Rasmussen, T., Rey, S.S., Myklebust, R., 2005. Seismic characteristics and distribution of volcanic intrusions and hydrothermal vent complexes in the Vøring and Møre basins. Pet. Geol. Conf. 2005 (6), 833e844.

Plaza-Faverola, A., Bünz, S., Johnson, J. E., Chand, S., Knies, J., Mienert, J., Franek. P., 2015. Role of tectonic stress in seepage evolution along the gas hydrate-charged Vestnesa Ridge, Fram Strait, Geophysical Research Letters, 42, 733–742, doi:10.1002/2014GL062474.

Procesi, M., Ciotoli, G., Mazzini, A., Etiope, G., 2019. Sediment-hosted geothermal systems: review and first global mapping. Earth Sci. Rev. 192, 529–544. https://doi.org/10.1016/j.earscirev.2019.03.020.

https://doi.org/10.5194/egusphere-2025-3487
Preprint. Discussion started: 16 September 2025

Sarhan, M., Safa, M., 2017. Application of Seismic Attributes for Detecting Different Geologic Features within Kafr El-Sheikh Formation, Temsah Concession, Nile Delta Basin. 7. 26-34. 10.21608/sjdfs.2017.194770.

Skogseid, J., Pedersen, T., Eldholm, O., Larsen, B.T., 1992. Tectonism and magmatism during NE Atlantic continental breakup: the Voring margin. Geological Society of London, 68 (1), 305–320. https://doi.org/10.1144/GSL.SP.1992.068.01.19.

Song, J., Alves, T., Omosanya, K., Tao, Z., 2020. Tectonic evolution of strike-slip zones on continental margins and their impact on the development of submarine landslides (Storegga Slide, Northeast Atlantic). Geological Society of America Bulletin. 132. 10.1130/B35421.1. DOI: 10.1130/B35421.1.

Souza, Z.S., Vasconcelos, P.M., Nascimento, M.A.L., Silveira, F.V., Paiva, H.S., Dias, L.G.S., 2004. Geocronologia e geoquímica do magmatismo cretácico a terciário no nordeste do Brazil. In: 42° Congresso Brasileiro de Geologia. Araxá, Abstracts CD, p. S32-T607.

Souza, Z.S., Wang, C., Jin, Z., Li, J., Yang, J., Botelho, N.F., Viana, R.R., Santos, L., Liu, P., Li, W., et al., 2019. Pyrometamorphic aureoles of Cretaceous sandstones and shales by Cenozoic basic intrusions, NE Brazil: Petrograhic, textural, chemical and experimental approaches. Lithos 326–327, 90–109. https://doi.org/10.1016/j.lithos.2018.11.033.

Svensen, H., Planke, S., Jamtveit, B., Pedersen, T., 2003. Seep carbonate formation controlled by hydrothermal vent complexes: a case study from the Voring Basin, the Norwegian Sea. Geo-Mar. Lett. 23 (3–4), 351–358. https://doi.org/10.1007/s00367-003-0141-2.

https://doi.org/10.5194/egusphere-2025-3487
Preprint. Discussion started: 16 September 2025

Svensen, H., Planke, S., Malthe-Sorenssen, A., Jamtveit, B., Myklebust, R., Eidem, T.R., Rey, S.S., 2004. Release of methane from a volcanic basin as a mechanism for initial Eocene global warming. Nature 429, 542–545. https://doi.org/10.1038/nature02566.

Svensen, H., Jamtveit, B., Planke, S., Chevallier, T., 2003. Structure and evolution of hydrothermal vent complexes in the Karoo Basin, South Africa. Journal of the Geological Society, London, Vol. 163, 2006, pp. 671–682.

Talukder, A. R., 2012. Review of submarine cold seep plumbing systems: leakage to seepage and venting. Terra Nova, 00, 1–18, doi: 10.1111/j.1365-3121.2012.01066.x.

Taner, M. T., Koehler, F., Sheriff R. E., 1976. Complex seismic trace analysis. Geophysics, 44 (6): 1041–1063. doi: https://doi.org/10.1190/1.1440994.

Wang, L., Sun, Z., Yang, J., Sun, Z., Zhu, J., Zhuo, H., Stock, J., 2019. Seismic characteristics and evolution of post-rift igneous complexes and hydrothermal vents in the Lingshui sag (Qiongdongnan basin), northwestern South China Sea, Marine Geology, V. 418, 106043, ISSN 0025-3227, https://doi.org/10.1016/j.margeo.2019.106043.

White, J.D.L., McClintock, M.K., 2001. Immense vent complex marks flood-basalt eruption in a wet, failed rift: Coombs Hills, Antarctica. Geological Society of America, v. 29; no. 10; p. 935–938;

Wu, R.-S., & Chen, L., 2006. Directional illumination analysis using beamlet decomposition and propagation. Geophysics, 71(4), S147–S159. doi:10.1190/1.2204963.

Wu, X., Liang, L., Shi, Y., Fomel, S., 2019b. FaultSeg3D: Using synthetic data sets to train an end-to-end convolutional neural network for 3D seismic fault

https://doi.org/10.5194/egusphere-2025-3487
Preprint. Discussion started: 16 September 2025

segmentation: Geophysics, 84, 35-45; http://dx.doi.org/10.1190/geo2018-0646.1.